# Efficient spin generation in graphene by magnetic proximity effect upon absorption of far-IR radiation

© K.S. Denisov, K.Yu. Golenitskii

Ioffe Institute,
194021 St. Petersburg, Russia
E-mail: denisokonstantin@gmail.com

Received May 2, 2023
Revised May 10, 2023
Accepted May 10, 2023

The magnetic proximity effect is significant for atomically thin layers of two-dimensional materials. In this paper, we study the mechanisms of photogeneration spin-polarized carriers in graphene on a magnetic insulator. The magnetic proximity effect and lowered symmetry at the interface enhance the spin response of graphene in the alternating electric field of the incident light. The first leads to spin splitting of the linear spectrum of Dirac electrons. The second increases the role of the spin-orbit interaction. The main mechanisms of photogenerated spin polarization have been considered, including spin flip intersubband and interband transitions, and their contribution to the absorption coefficient of graphene.

**Keywords:** Dirac electrons, graphene, electric dipole spin resonance, spin-orbit coupling, spin generation.

DOI: 10.21883/SC.2023.03.56234.4756

## 1. Introduction

An important feature of atomically thin layers of two-dimensional materials such as graphene, dichalcogenides, and transition metal carbides (TMDs and MXenes) is the high susceptibility of their physical properties to the external environment. Atomically thin materials experience a noticeable proximity effect due to interaction with adjacent materials, which can be used to deliberately change their properties and create heterostructures with new characteristics [1–3]. For example, when forming structures based on superconducting compounds and graphene layers, induced superconductivity [4] can occur in the latter. The dielectric environment plays an important role for the optical properties and exciton structure of transition metal dichalcogenides [5,6]. In case of magnetic layers, there is a partial hybridization of the states of a magnet and a two-dimensional semiconductor at the interface, the so-called *magnetic proximity effect*. It leads to the Zeeman splitting of the spin states of two-dimensional charge carriers and the formation of an equilibrium spin polarization in a two-dimensional layer [7,8].

Recently, graphene-based heterostructures on magnetic materials (G/M) [1] have obtained particular importance. Significant progress is observed in the fabrication of G/M structures using magnetic substrates of various chemical compositions. A significant magnetic proximity effect in G/M has been demonstrated using ferromagnetic metals [8–12], magnetic insulators [7,13–15], antiferromagnets [16,17] and monolayers of two-dimensional magnets [18–22]. On the other hand, the understanding of the physics of the magnetic proximity effect, the nature of the hybridization of wave functions, and the modification of the spectrum of two-dimensional electrons, taking into account new spin-dependent ones in the effective Hamiltonian [1,3,15], has significantly expanded.

Historically, studies of graphene in G/M structures have been associated with the so-called *K*-point spin filtering [23,24], which causes selective transmission of spin polarization through the graphene layer. This effect is considered to be a promising method for increasing the efficiency of spin injection in devices based on the effect of tunneling magnetoresistance (TMR) [25]. To date, it has been established that the properties of such contacts strongly depend on the structure of the interface between graphene and a ferromagnet. In particular, when a strong covalent bond is formed at the interface, the initial band structure of graphene is practically practically lost, and the bulk states of the ferromagnet have a dominant effect on the electronic spectrum in graphene [24]. On the contrary, if the structure contains an intermediate dielectric tunneling barrier [8,26], then the spin splitting is observed without the suppression of the Dirac cones.

The linear electronic spectrum in graphene is also preserved when placed on magnetic insulators, here the magnetic proximity effect manifests itself due to the exchange interaction with the substrate. Recently the appearance of spin polarization of Dirac electrons was demonstrated in graphene with a Zeeman splitting of up to several meV (EuS [7], YIG [14], CrBr3 [19]) and tens of meV [27] (CrSBr [16], CrSe [17]). In addition, there are a number of papers, the authors of which indicate the opportunity of controlling spin splitting by technological [22,27,28] and electrical methods [26,29].

G/M heterostructures seem promising for improving the functionality of devices using the TMR effect [25], and the electrical and tunneling properties of similar structures are being actively studied. Meanwhile, much less is known

about the physics of optically induced spin phenomena in graphene under conditions of the magnetic proximity effect. Symmetry reduction due to the presence of an interface and partial hybridization between the electron states in graphene and in the magnetic substrate are additionally accompanied by an increase in the spin-orbit interaction (SOI), which is described by various spin-dependent contributions in the effective Hamiltonian [3,15,30–33]. Optical studies of G/M structures are important for understanding the physics of spin phenomena under the conditions of a complex magnetic proximity effect, but today they are practically not presented. Additionally, studies of optically induced spin phenomena in two-dimensional nanostructures seem to be important for optoelectronic devices using spin polarization of carriers [34,35].

The presence of spin-orbit terms in the Hamiltonian enhances spin-flip optical transitions similar to the effect of enhancement of spin susceptibility as a result of electric dipole spin resonance [36–38]. Previously, the effects of spin generation in graphene under optical irradiation were studied in papers [39,40]. In the [39] spin photogeneration was due to Rashba spin-orbit interaction, which has a spatially inhomogeneous random structure with zero mean value. This mechanism depends on the correlation function of the random spin-orbit potential and is relevant for non-planar graphene layers with „ripples“. The paper [40] considered a strong spin-orbit coupling, when the spectrum of graphene becomes parabolic for small wave vectors. In both works, nonmagnetic structures were studied in the Voigt geometry, when the external magnetic field vector is parallel to the graphene plane.

In this paper, we study various microscopic mechanisms of spin photogeneration in graphene located on a magnetic insulator substrate. It is assumed that the linear electronic spectrum is preserved upon contact with a magnetic substrate. In contrast, the effect of the latter will consist in the appearance of a spin splitting, the magnitude of which can reach several meV, which agrees with experimental observations in structures with graphene [3,31,32]. In contrast to the papers [39,40], we will assume that the spin-orbit interaction is small compared to the Zeeman splitting due to the exchange interaction with the substrate, and the magnetization orientation is perpendicular to graphene. Such a case is specific for magnetic heterostructures: the equilibrium spin polarization of Dirac electrons, oriented perpendicularly, cannot be realized in nonmagnetic structures using an external magnetic field without the simultaneous formation of Landau levels.

In this paper, we consider the main mechanisms of spin photogeneration in graphene due to an alternating electric field and taking into account various interface contributions to the spin-orbit interaction. The mechanisms of spin generation for intersubband absorption are analyzed. It is shown that the presence of momentum-independent contributions to SOI additionally leads to interband spin-flip transitions. These processes are important in a wide spectral range (from several to tens of meV), while their influence on the total absorption factor can reach 10% with the efficiency of spin photogeneration up to several percent.

## 2. Effective Hamiltonian

We use the model of the effective Hamiltonian of Dirac electrons $H = H_0 + H_{ex} + H_{so}$, where

$$H_0 = v_F (\kappa\sigma_x k_x + \sigma_y k_y) \quad (1)$$

— standard Hamiltonian of electrons in graphene. Here $v_F \approx 10^8$ cm/s — the Fermi velocity in graphene, the momentum $\mathbf{k}$ is measured relative to the points $(K, K')$ of the Brillouin zone ($\kappa = +1$ refers to the valley $K$, and $\kappa = -1$ to $K'$), $\boldsymbol{\sigma}$ — a vector of Pauli matrices describing the pseudospin. Units of measurement are selected so that $\hbar = 1$. The term $H_{ex}$ takes into account the spin splitting due to the proximity effect and exchange interaction with the magnetic substrate

$$H_{ex} = \Delta_{ex}(\mathbf{n} \cdot \mathbf{s}). \quad (2)$$

Here $\mathbf{s}$ — electron spin operator, $\mathbf{n}$ — unit vector directed along the substrate magnetization.

The remaining part of the effective Hamiltonian $H_{so}$ contains various contributions from the spin-orbit interaction and essentially depends on the symmetry of the system, the type of substrate, and its chemical composition [30–33]. In paper, we will focus on the Bychkov–Rashba [15,18,41–43] mechanism associated with the absence of $z \to -z$ reflective symmetry at the interface (a specific mechanism may be associated with the appearance of a transverse electric field or the substrate effect). The first non-vanishing terms of the $\mathbf{k}$-expansion expansion of $H_{so}$ are described by two constants $\lambda_1$ and $\lambda_2$:

$$H_{so} = \lambda_1 (\kappa\sigma_x s_y - \sigma_y s_x) + \lambda_2 a_0 (k_x s_y - k_y s_x), \quad (3)$$

where $a_0 = 0.24$ nm — graphene lattice constant. It is important to note that the first term does not depend on the momentum of the electron $\mathbf{k}$. Such a contribution is specific to systems with a linear spectrum and will play a particularly important role in our further consideration.

We neglect the intrinsic spin-orbit interaction of the Kane–Mele [44] type, since for graphene it turns out to be much smaller than the considered contributions. In addition, we will not consider the effects associated with the breaking of symmetry between the graphene two sub-lattices. They can occur when graphene lies on a less symmetrical substrate. On the whole, this leads to the opening of a gap in the spectrum and to the appearance of additional contributions to the spin-orbit interaction [31,34,45,46]. Let us note that these mechanisms apparently have a significant effect on the spin phenomena in structures based on graphene and TMDs [31,34,45,47].

In contrast to traditional two-dimensional electronic systems, for example, GaAs-based quantum wells, spin splittings in graphene on magnetic substrates turn out to

be quite large in absolute value and lie in the region of several meV [1,3,32] (in contrast to tens of $\mu$eV for SOI splitting in GaAs quantum wells [48]). This circumstance qualitatively indicates a potential enhancement of the effects of spin generation upon absorption of light, if the induced spin-orbit interaction is involved in this case.

## 3. Optical transitions

Let us consider the absorption of light by electrons in the $K$-valley. For the valley $K'$ the consideration is similar, and the final expression is multiplied by 2 (valley splitting is not taken into account). The contribution $H_{\text{int}}$ to the Hamiltonian from the interaction of electrons with an electromagnetic wave is obtained using the minimal coupling $\mathbf{k} \to \mathbf{k} - (e/c)\mathbf{A}$, where $\mathbf{A}$ — the vector potential of the wave

$$H_{\text{int}} = -\frac{e}{c}\left(v_{\text{F}}\,(\boldsymbol{\sigma}\mathbf{A}) + \lambda_2 a_0\,[\mathbf{A}\times\mathbf{s}]\,\mathbf{e}_z\right), \qquad (4)$$

where $\mathbf{e}_z$ — the unit vector of the normal to the graphene plane. In the chosen gauge we have $\mathbf{A}_\omega = -(ic/\omega)\mathbf{E}_\omega$ and $\phi = 0$. When the spin-orbit interaction is taken into account, transitions with spin flip under the action of the electric component of the field become allowed, i.e., in the electric dipole approximation. In the system under consideration, the magnetic dipole transitions are several orders of magnitude weaker, and we neglect it.

We will assume that the spin-orbit contributions are small compared to the characteristic kinetic energy of the electron and therefore can be taken into account in the framework of perturbation theory. Meanwhile, the spin splitting due to the exchange interaction and the magnetic proximity effect are not assumed to be small, implying $\Delta_{\text{ex}} \gg H_{\text{so}}$. Therefore, the electron dispersion can be considered almost linear $\varepsilon_{k,\pm,s} = \pm v_{\text{F}}k + \Delta_{\text{ex}}s$ and representing two cones separated by an energy $\Delta_{\text{ex}}$, where $s = \pm 1/2$ is the spin projection on the magnetization axis. Wave functions of an electron, unperturbed $H_{\text{so}}$, can be represented as $\psi^0_{k\mu s} = e^{i\mathbf{kr}}u^0_{k\mu s}$, where $\mu = \pm$ and $u^0_{k\mu s}$ has the form

$$\left|u^0_{k\mu s}\right\rangle = \frac{1}{\sqrt{2}}\begin{pmatrix}1\\ \mu e^{i\varphi}\end{pmatrix}|s\rangle. \qquad (5)$$

Here $\varphi$ — angle between $\mathbf{k}$ momentum direction and axis $x$, $|s\rangle$ — spin eigenstate of operator $H_{\text{ex}}$.

The scheme of vertical optical transitions in this system is shown in Fig. 1. Here and below, it is assumed that the momentum of the electron is conserved during the transition between different states, and only the normal incidence of the electromagnetic wave is considered. The first term in $H_{\text{int}}$ (4) is not directly related to the spin operator and leads primarily to interband transitions without spin flip. These processes are responsible for the universal absorption in graphene at zero temperature, at which the absorption coefficient $\alpha_0 = \pi e^2/\hbar c \approx 2.3\%$ turns out to be frequency independent and is determined by the fine structure constant.

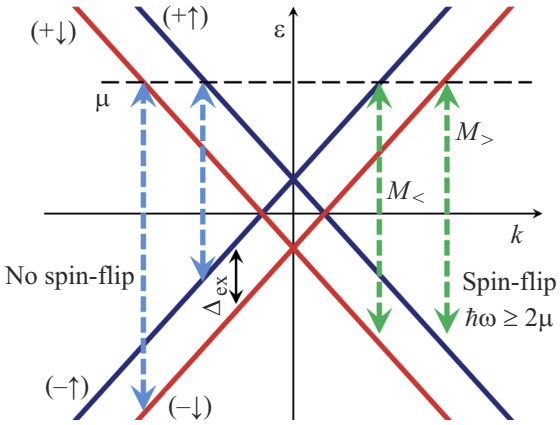


**Figure 1.** Electron energy spectrum $\varepsilon(k)$ and scheme of interband optical transitions in graphene on a magnetic substrate taking into account the proximity effect. $\Delta_{\text{ex}}$ — spin splitting value, $\mu$ — Fermi level in graphene. Arrows on the right — spin flip transitions. Arrows on the left — transitions without spin flip.

The second term in $H_{\text{int}}$ (4) is coupled with the electron spin operator. Accounting for this contribution leads to intersubband transitions with spin flip similar to the electron spin resonance scheme. The term $\propto \lambda_2[\mathbf{e}_z \times \mathbf{A}]$ acts as an alternating magnetic field. To describe the transition in the first order in $H_{\text{so}}$, it is sufficient to take the unperturbed wave function from expression (5). The matrix element of the vertical transition between the states of two Dirac cones ($\mu = +1$) with different spin projections on the $\mathbf{n}$ axis is given by

$$N^p_+ = -\frac{e}{c}\lambda_2 a_0 A^p_\omega\,\left\langle u^0_{k+\uparrow}\right|\hat{\mathbf{s}}\cdot(\mathbf{e}_z\times\mathbf{o}_p)\left|u^0_{k+\downarrow}\right\rangle, \qquad (6)$$

where $\mathbf{o}_p$ — the unit polarization of light, by definition $\mathbf{A}_\omega = A^p_\omega\mathbf{o}_p$, the index $p$ determines the polarization of the wave. It is important to note that transitions in this scheme can only occur between the upper spin-split cones (or the lower cones in the case of $p$-doping of graphene), since the contribution from $\lambda_2$ to the velocity operator does not explicitly contain either pseudospin or momentum. The resonant frequency of intersubband absorption turns out to be constant $\hbar\omega = \Delta_{\text{ex}}$, and the square of the matrix element does not depend on the direction of the electron momentum $|N^p_+|^2 \propto (\lambda_2 a_0/v_{\text{F}})^2$.

The spin-orbit contributions to $H_{\text{so}}$, which do not depend on the electron momentum, do not directly affect the form of $H_{\text{int}}$, as happens in the case of linear in momentum terms. However, their presence also leads to spin photogeneration, so that spin-flip absorption can take place both for intersubband and interband transitions, which is noted in Fig. 1. Optical transitions are excited in this case by the first term in $H_{\text{int}}$, while processes with spin flip arise from a change in the wave functions of the electron when $H_{\text{so}}$ is taken into account. This mechanism is specific for systems with

a Dirac spectrum; the effect of spin photogeneration during interband absorption was previously considered in [40].

Let us present in more detail the calculation of interband matrix elements of spin-flip absorption. As can be seen from Fig. 1, two such processes are possible; they differ in the projection of the spin in the final state. The corresponding matrix elements will be denoted as $M_<$ for the transition $(-\downarrow) \to (+\uparrow)$ and $M_>$ for the transition $(-\uparrow) \to (+\downarrow)$. To simplify the calculations, we will consider the case $\mathbf{n} = \mathbf{e}_z$, when the magnetization orientation is normal to the graphene plane. The generalization of the calculation to the case of an arbitrary orientation of $\mathbf{n}$ is straightforward.

The general expression is as follows

$$M_\gamma^p = -\frac{e}{c} A_\omega^p (\mathbf{o}_p \cdot \mathbf{v}_\alpha), \quad \gamma = \{>, <\}, \tag{7}$$

where, for instance, $\mathbf{v}_\alpha = \langle u_{k+\uparrow} | v_F \boldsymbol{\sigma} | u_{k-\downarrow} \rangle$ — the matrix element of the velocity operator $\mathbf{v} = v_F \boldsymbol{\sigma}$ calculated on the exact amplitudes of the wave functions $u_{k\mu s}$ taking into account $H_{so}$. To obtain $M^p_{>,<}$, we use the formula for changing the wave functions in the first order of perturbation theory with respect to $H_{so}$. The unperturbed Hamiltonian is $H_0 + H_{ex}$, while the spectrum of the system $\varepsilon_{k,\pm,s} = \pm v_F k + \Delta_{ex} s$ and wave functions are given (5). Taking into account the matrix $H_{so}$, we have

$$\delta u_{k\mu s} = \sum_{\nu=\pm} \frac{H_{so}^{(\nu s';\mu s)}}{\varepsilon_{k\mu s} - \varepsilon_{k\nu s'}} \left| u^0_{k\nu s'} \right\rangle, \qquad s' \neq s, \tag{8}$$

where the matrix elements

$$H_{so}^{(+\uparrow;+\downarrow)} = H_{so}^{(+\uparrow;-\downarrow)} = -\frac{i\lambda_1}{2} e^{-i\varphi},$$

$$H_{so}^{(-\uparrow;+\downarrow)} = H_{so}^{(-\uparrow;-\downarrow)} = \frac{i\lambda_1}{2} e^{-i\varphi}.$$

Let us extract the dimensionless factor $\widetilde{M}^p_\gamma$ related to the wave polarization in explicit form from $M^p_\gamma$. For example, $M^x_\gamma = (e/c) v_F A^x_\omega \widetilde{M}^x_\gamma$ in case of linear polarization $\mathbf{o}_p = \mathbf{e}_x$. In the first order by $\lambda_1$

$$\widetilde{M}^x_{>,<} = \pm i\lambda_1 \frac{\Delta_{ex} \pm v_F k \left(1 - e^{\mp 2i\varphi}\right)}{\Delta_{ex}(\Delta_{ex} \pm 2 v_F k)}, \tag{9}$$

where for $>$ it is necessary to take the upper sign, and for $<$ — the lower one.

It should be noted that at $v_F k \gg \Delta_{ex}$ the probability of interband transitions is approximately equal to $|\widetilde{M}^x_\gamma|^2 \approx (\lambda_1/\Delta_{ex})^2 \sin^2\varphi$. The momentum distribution of photoexcited electrons is determined by the square of the absorption matrix element. The anisotropic dependence of the absorption probability on the angle $\varphi$ can lead to alignment of carriers in momentum — linearly polarized light excites charge carriers anisotropically distributed in momentum space. As the momentum $k$ decreases, the angular distribution of $|\widetilde{M}^x_\gamma|^2$ becomes more isotropic, which is shown in the dependences $|\widetilde{M}^x_\gamma(\varphi)|^2$ in Fig. 2 for various

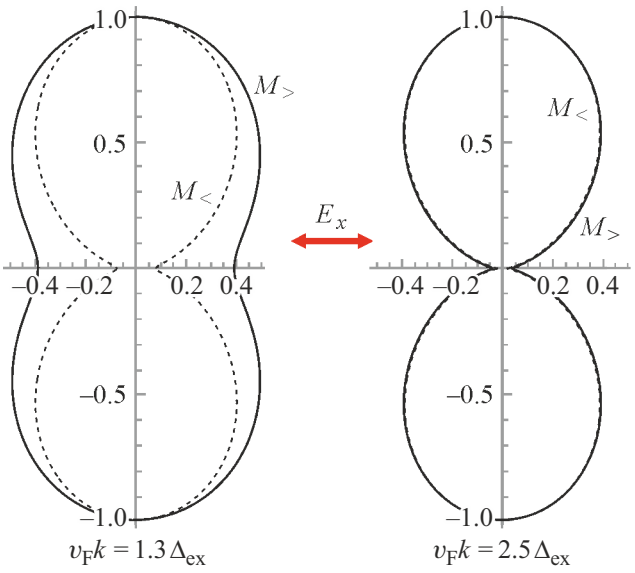


**Figure 2.** Angular distribution of the probability of light spin-flip absorption for two interband transitions $M_{>,<}$ at different ratios $v_F k/\Delta_{ex}$. The orientation of the electric field of a linearly polarized wave is shown by the red arrow.

ratios $v_F k/\Delta_{ex}$. It should be noted that in the $vk \gg \Delta_{ex}$ region the averaged square of the absorption matrix element $\left\langle |\widetilde{M}^p_\gamma|^2 \right\rangle$ turns out to be independent of the radiation polarization. This circumstance is due to the specific structure of $H_{so}$ and the term $\lambda_1$, which does not depend on the electron momentum.

The matrix element of spin-flip intersubband transitions is calculated in a similar way. The final result for a linearly polarized wave $\mathbf{o}_p = \mathbf{e}_x$ for the conduction band the form

$$\widetilde{M}^x_+ = i\lambda_1 \frac{v_F k \left(1 - e^{-2i\varphi}\right)}{\Delta_{ex}^2 - (2 v_F k)^2}. \tag{10}$$

This transition leads to absorption at the same resonant frequency as in the situation with the $\lambda_2$ — mechanism ($\hbar\omega = \Delta_{ex}$). In the region $v_F k \gg \Delta_{ex}$, however, the square of the matrix element obtains an additional small factor $|\widetilde{M}^x_+|^2 \propto (\lambda_1/v_F k)^2 \sin^2\varphi$. Thus, one should expect suppression of this mechanism when the Fermi level is $\mu \gg \Delta_{ex}$, to the extent of the parameter $(\lambda_1/\mu)^2$ compared to interband transitions. The polarization dependence of $\langle |\widetilde{M}^p_+|^2 \rangle$ is also absent in the case of intersubband transitions.

## 4. Spin photogeneration

The absorption factor is related to the longitudinal optical conductivity $\alpha(\omega) = (4\pi/c)\,\mathrm{Re}\,[\sigma_{xx}(\omega)]$ and is equal in the general case

$$\alpha = \frac{4\pi^2 e^2}{\omega c A} \sum_{k,\beta,\beta'} (f_{k\beta} - f_{k\beta'}) \left| v^x_{\beta\beta'} \right|^2 \delta(\varepsilon_{k\beta'} - \varepsilon_{k\beta} + \hbar\omega), \tag{11}$$

where index $\beta = (\mu, s)$ includes orbital states $\mu = \pm 1$ and various spin projections, $f_{k\beta}$ — equilibrium distribution function, $A$ — sample area, $v^x_{\beta\beta'}$ — matrix element of velocity operator $v = \partial H/\partial k$. Expression (11) includes spin-flip processes. Next, we consider the case of zero temperature $T = 0$ and $n$-doping of graphene, when the electrons are degenerate and fill part of the Dirac cone in both spin sub-bands, with the Fermi level $\mu > \Delta_{ex}$.

It is convenient to represent the total absorption factor as the sum of several terms corresponding to different transitions:

$$\alpha_{total} = \alpha_\uparrow + \alpha_\downarrow + \alpha_{is} + \alpha_{inter}. \tag{12}$$

Here $\alpha_{\uparrow,\downarrow}$ corresponds to interband absorption inside the spin sub-bands separately. This contribution has the form of $\alpha_{\uparrow,\downarrow} = (\alpha_0/2)\Theta(\hbar\omega - 2\mu_{\uparrow,\downarrow})$, where $\mu_{\uparrow,\downarrow} = \mu \mp \Delta_{ex}/2$ and $\Theta$ — Heaviside function. In the frequency range $\hbar\omega > 2\mu + \Delta_{ex}$ we have the contribution of the universal absorption $\alpha_\uparrow + \alpha_\downarrow = \alpha_0$.

The terms $\alpha_{is}$ and $\alpha_{inter}$ refer to spin-flip absorption processes and describe intersubband and interband transitions, respectively. To calculate intersubband processes in the upper Dirac cone, it is necessary to consider the terms in (11) with indices $\beta = (+, \uparrow)$ and $\beta' = (+, \downarrow)$. Intersubband absorption is centered at the frequency $\omega = \Delta_{ex}/\hbar$ and has an $\delta$-shaped form. The characteristic resonant frequencies $\omega$ are in the terahertz range. For momentum-independent contributions to $H_{so}$ we have

$$\alpha_{is} \approx \alpha_0 \frac{\lambda_1^2}{2\mu} \delta(\hbar\omega - \Delta_{ex}). \tag{13}$$

We note that in a situation where both mechanisms of the Bychkov–Rashba spin-orbit interaction in (3) turn out to be approximately of the same magnitude, the interference contribution between them must be taken into account. The width of the intersubband line is determined by the mechanisms of transverse spin relaxation, which also significantly affects the final efficiency of spin photogeneration.

The interband absorption $\alpha_{inter}$ has a different frequency dependence, let us consider it in more detail. As discussed in the previous section, there are two interband processes, which are described by matrix elements $M^x_{>,<}$ in accordance with (9). We separate the contributions from these channels in $a_i = \alpha_> + \alpha_<$. Spin splitting preserves the electron-hole symmetry of the spectrum, so that for processes with spin flip (see Fig. 1) at zero temperature, absorption in both channels is possible for the radiation energy $\hbar\omega \geq 2\mu$. To calculate these contributions to (11), it is necessary to consider the indices $\beta = (+\downarrow)$, $\beta' = (-\uparrow)$ and $\beta = (+\uparrow)$, $\beta' = (-\downarrow)$ for $M^x_{>,<}$ respectively. Using (9), the calculation of the sum can be carried out and analytical expressions can be obtained

$$\alpha_{>,<} = \frac{\alpha_0}{4}\lambda_1^2 \left(1 \pm \frac{\Delta_{ex}}{\hbar\omega}\right)\left(\frac{1}{\Delta_{ex}^2} + \frac{1}{(\hbar\omega)^2}\right)\Theta(\hbar\omega - 2\mu), \tag{14}$$

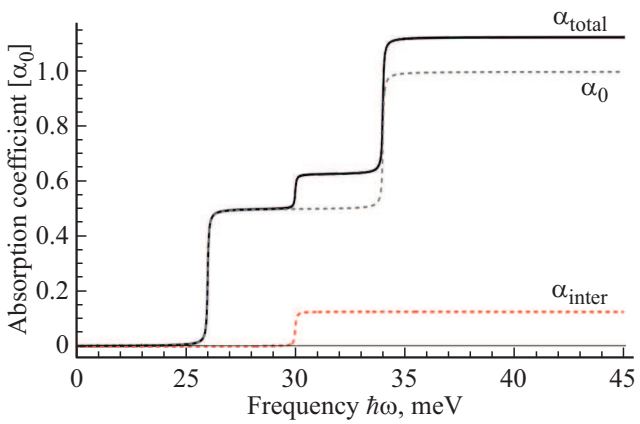


**Figure 3.** Frequency dependence of the absorption factor in the region of interband transitions and the efficiency of nonequilibrium spin photogeneration. Parameters: $\mu = 15$ meV, $\Delta_{ex} = 4$ meV, $\lambda_1 = 2$ meV.

where plus corresponds to $<$ and minus — to $>$. The given formulas are valid when $\mu > \Delta_{ex}/2$. At smaller $\mu$, it is important to take into account the transitions $(+\downarrow) \to (-\uparrow)$, while the denominator in (8) can become zero, for example, under the condition $\varepsilon_{k,+,\downarrow} - \varepsilon_{k,-,\uparrow} = 2kv_F - \Delta_{ex} = 0$. In this region of wave vectors, the perturbation theory is not applicable, and the corrections must be calculated in a different way, for example, by performing an exact diagonalization of the complete Hamiltonian. Here we do not consider this situation and assume that $2kv_F \neq \Delta_{ex}$.

The final expression for the interband contribution to the absorption factor

$$\alpha_{inter} = \frac{\alpha_0}{2}\lambda_1^2 \left(\frac{1}{\Delta_{ex}^2} + \frac{1}{(\hbar\omega)^2}\right)\Theta(\hbar\omega - 2\mu). \tag{15}$$

In the $\mu \gg \Delta_{ex}$ limit, it does not depend on the frequency and is equal to $(\alpha_0/2)(\lambda_1/\Delta_{ex})^2$. From the papers [7,31] we took estimates of the quantities that determine the spin splittings, $\Delta_{ex} = 4$ meV and $\lambda_1 = 2$ meV, and the Fermi energy $\mu = 15$ meV.

Figure 3 shows the spectrum of the total absorption coefficient and the contributions from specific processes with the conservation and change of spin in the frequency range corresponding to interband transitions. For the selected parameters, the dispersion of $\alpha_{inter}$ is practically absent. The stepped character of $\alpha_{total}$ is related to the spin splitting of the Dirac cones. Universal absorption for each Dirac cone starts with a different energy $\hbar\omega$, and the distance between the energies is $2\Delta_{ex}$ (Fig. 1). In addition, in the $\mu \gg \Delta_{ex}$ limit, the relative role of transitions with spin flip

$$\frac{\alpha_{inter}}{\alpha_{total}} \approx \frac{\lambda_1^2}{2\Delta_{ex}^2}. \tag{16}$$

For the chosen parameters we estimate this ratio $\approx 12\%$. Strictly speaking, the obtained value should be considered the upper estimate, since in this case $\lambda_1/\Delta_{ex} = 0.5$ and, accordingly, the perturbation theory is not accurate.

To estimate the efficiency of spin photogeneration, we define the degree of optical orientation $P$ as the ratio of the difference between the absorption factors for processes with different spins to the total absorption factor $P = (\alpha_> - \alpha_<)/\alpha_{\text{total}}$. This value shows the fraction of photoexcited electrons with opposite spin polarization relative to the total number of photoexcited electrons in the upper Dirac cones. In the $\mu \gg \Delta_{\text{ex}}$ limit, the degree of optical orientation

$$P \approx \frac{\lambda_1^2}{2\Delta_{\text{ex}}\hbar\omega} \tag{17}$$

decreases with increasing frequency of $P \propto \omega^{-1}$. With the ration $\Delta_{\text{ex}}/\mu \approx 0.25$ we obtain $P \approx 3\%$.

## 5. Possible experimental observation

The absorption factor of atomically thin materials can be measured with sufficiently high accuracy by optical methods, for example, when studying the reflectance from a heterostructure [49,50]. Usually the optical contrast is measured $\delta_R = |R - R_g|$, i.e. relative difference between the reflectances from the substrate with graphene $R_g$ and without it $R$. If $n_s$is the refractive index of the substrate and the absorption in graphene is small, then the following relation is valid:

$$\delta_R \approx \frac{4\alpha_{\text{total}}}{n_s^2 - 1}. \tag{18}$$

By forming additional dielectric layers on graphene, the optical contrast can be increased, which will allow to measure finer contributions to absorption [51]. Moreover, ultrasensitive schemes for optical studies of two-dimensional materials, including those in the terahertz range, based on the use of a substrate as a Fabry–Perot interferometer, are currently being developed. The application of such experimental techniques opens up the opportunity of direct optical detection of the effect of spin photogeneration during interband transitions under conditions when its efficiency reaches at least 5−10%, and it seems possible to distinguish the contribution of $\alpha_{\text{inter}}$ from the background of random noise [49,50]. Additionally, the frequency-independent contribution of $\alpha_{\text{inter}}$ to spin-flip processes with suppressed $\lambda_2$-should, in theory, manifest itself up to the near infrared range. Let us note that to observe the spectral features of the absorption factor shown in Fig. 3 (in a lower frequency range), low temperatures and rather high electron mobilities in graphene are required. The reciprocal scattering time in energy units should not exceed a few meV; otherwise, the response of interest can be masked by Drude absorption.

As an alternative to direct optical measurements, a scheme for electrical detection of nonequilibrium spin polarization in graphene using ferromagnetic contacts [52] and the Johnson–Silsbee effect [53] can be used. The advantage of this technique may lie in the fact that the photovoltage is determined mainly by the nonequilibrium spin polarization of electrons in graphene, which arises only in the processes of spin photogeneration.

## 6. Conclusion

The processes of photogeneration of spin-polarized charge carriers in graphene structures on a magnetic insulator substrate were studied in this paper. The main mechanisms of spin photogeneration under conditions of a strong magnetic proximity effect and symmetry reduction at the interface with the substrate are considered. It is shown that taking into account the momentum-independent terms responsible for the spin-orbit interaction in the Hamiltonian for electrons in graphene leads to the appearance of new channels for the generation of spin-polarized carriers during interband absorption of light in the far-IR frequency range. It was predicted that, for realistic parameters, spin-flip transitions can make a significant contribution to the total absorption coefficient, with the degree of optical spin orientation reaching several percent. The results obtained can be used for experimental studies of the magnetic proximity effect in structures based on two-dimensional materials, as well as for the development of optoelectronic devices using the spin polarization of charge carriers in conducting channels.

### Acknowledgments

The authors express gratitude to I.V. Rozhanskii and N.S. Averkiev (Ioffe Institute) for useful scientific discussions.

### Funding

The paper was carried out as part of project No. 22-22-20082 (Russian Science Foundation agreement No. 22-22-20082 dated 25.03.2022, regional grant agreement No. 23/2022 dated 14.04.2022)).

### Conflict of interest

The authors declare that they have no conflict of interest.

## References

[1] I. Žutić, A. Matos-Abiague, B. Scharf, H. Dery, K. Belashchenko. Mater. Today, **22**, 85 (2019).
[2] K. Tran, G. Moody, F. Wu, X. Lu, J. Choi, K. Kim, A. Rai, D.A. Sanchez, J. Quan, A. Singh, J. Embley, A. Zepeda, M. Campbell, T. Autry, T. Taniguchi, K. Watanabe, N. Lu, S.K. Banerjee, K.L. Silverman, S. Kim, E. Tutuc, L. Yang, A.H. MacDonald, X. Li. Nature, **567** (7746), 71 (2019).
[3] J.F. Sierra, J. Fabian, R.K. Kawakami, S. Roche, S.O. Valenzuela. Nature Nanotechnol., **16** (8), 856 (2021).
[4] D.K. Efetov, L. Wang, C. Handschin, K.B. Efetov, J. Shuang, R. Cava, T. Taniguchi, K. Watanabe, J. Hone, C.R. Dean, P. Kim. Nature Physics, **12** (4), 328 (2015).
[5] G. Wang, A. Chernikov, M.M. Glazov, T.F. Heinz, X. Marie, T. Amand, B. Urbaszek. Rev. Mod. Phys., **90** (2) (2018).

[6] F. Cadiz, E. Courtade, C. Robert, G. Wang, Y. Shen, H. Cai, T. Taniguchi, K. Watanabe, H. Carrere, D. Lagarde, M. Manca, T. Amand, P. Renucci, S. Tongay, X. Marie, B. Urbaszek. Phys. Rev. X, **7** (2) (2017).
[7] P. Wei, S. Lee, F. Lemaitre, L. Pinel, D. Cutaia, W. Cha, F. Katmis, Y. Zhu, D. Heiman, J. Hone, J.S. Moodera, C.-T. Chen. Nature Materials, **15** (7), 711 (2016).
[8] P.U. Asshoff, J.L. Sambricio, A.P. Rooney, S. Slizovskiy, A. Mishchenko, A.M. Rakowski, E.W. Hill, A.K. Geim, S.J. Haigh, V.I. Fal'ko, I.J. Vera-Marun, I.V. Grigorieva. NPJ 2D Mater., **4** (3), 031004 (2017).
[9] E. Cobas, A.L. Friedman, O.M.J. van't Erve, J.T. Robinson, B.T. Jonker. Nano Lett., **12** (6), 3000 (2012).
[10] A. Dahal, M. Batzill. Nanoscale, **6** (5), 2548 (2014).
[11] M. Cattelan, G.W. Peng, E. Cavaliere, L. Artiglia, A. Barinov, L.T. Roling, M. Favaro, I. Píš, S. Nappini, E. Magnano, F. Bondino, L. Gavioli, S. Agnoli, M. Mavrikakis, G. Granozzi. Nanoscale, **7** (6), 2450 (2015).
[12] W.Q. Liu, W.Y. Wang, J.J. Wang, F.Q. Wang, C. Lu, F. Jin, A. Zhang, Q.M. Zhang, G. van der Laan, Y.B. Xu, Q.X. Li, R. Zhang. Sci. Rep., **5** (1), 1 (2015).
[13] A.G. Swartz, P.M. Odenthal, Y. Hao, R.S. Ruoff, R.K. Kawakami. ACS Nano, **6** (11), 10063 (2012).
[14] Z. Wang, C. Tang, R. Sachs, Y. Barlas, J. Shi. Phys. Rev. Lett., **114**, 016603 (2015).
[15] B. Karpiak, A.W. Cummings, K. Zollner, M. Vila, D. Khokhriakov, A.M. Hoque, A. Dankert, P. Svedlindh, J. Fabian, S. Roche, S.P. Dash. NPJ 2D Mater., **7** (1), 015026 (2019).
[16] T.S. Ghiasi, A.A. Kaverzin, A.H. Dismukes, D.K. de Wal, X. Roy, B.J. van Wees. Nature Nanotechnol., **16** (7), 788 (2021).
[17] Y.Wu, G. Yin, L. Pan, A.J. Grutter, Q. Pan, A. Lee, D.A. Gilbert, J.A. Borchers, W. Ratcliff, A. Li, X. dong Han, K.L. Wang. Nature Electron., **3** (10), 604 (2020).
[18] K. Zollner, M. Gmitra, J. Fabian. New J. Phys., **20** (7), 073007 (2018).
[19] C. Tang, Z. Zhang, S. Lai, Q. Tan, W.-b. Gao. Adv. Mater., **32** (16), 1908498 (2020).
[20] B. Zhou, S. Ji, Z. Tian, W. Cheng, X. Wang, W. Mi. Carbon, **132**, 25 (2018).
[21] M.U. Farooq, J. Hong. NPJ 2D Mater. Appl., **3** (1), 1 (2019).
[22] K. Zollner, M.D. Petrović, K. Dolui, P. Plecháč, B.K. Nikolić, J. Fabian. Phys. Rev. Res., **2** (4), 043057 (2020).
[23] V.M. Karpan, G. Giovannetti, P.A. Khomyakov, M. Talanana, A.A. Starikov, M. Zwierzycki, J. van den Brink, G. Brocks, P.J. Kelly. Phys. Rev. Lett., **99**, 176602 (2007).
[24] V.M. Karpan, P.A. Khomyakov, A.A. Starikov, G. Giovannetti, M. Zwierzycki, M. Talanana, G. Brocks, J. van den Brink, P.J. Kelly. Phys. Rev. B, **78** (19) (2008).
[25] J.-F. Dayen, S.J. Ray, O. Karis, I.J. Vera-Marun, M.V. Kamalakar. Appl. Phys. Rev., **7** (1), 011303 (2020).
[26] J. Xu, S. Singh, J. Katoch, G. Wu, T. Zhu, I. Žutić, R.K. Kawakami. Nature Commun., **9** (1), 1 (2018).
[27] C. Tang, B. Cheng, M. Aldosary, Z. Wang, Z. Jiang, K. Watanabe, T. Taniguchi, M. Bockrath, J. Shi. APL Mater., **6** (2), 026401 (2018).
[28] H.X. Yang, A. Hallal, D. Terrade, X. Waintal, S. Roche, M. Chshiev. Phys. Rev. Lett., **110**, 046603 (2013).
[29] P. Lazić, K.D. Belashchenko, I. Žutić. Phys. Rev. B, **93** (24), 241401 (2016).
[30] W. Han, R.K. Kawakami, M. Gmitra, J. Fabian. Nature Nanotechnol., **9** (10), 794 (2014).
[31] J.H. Garcia, M. Vila, A.W. Cummings, S. Roche. Chem. Soc. Rev., **47** (9), 3359 (2018).
[32] A. Avsar, H. Ochoa, F. Guinea, B. Özyilmaz, B.J. van Wees, I.J. Vera-Marun. Rev. Mod. Phys., **92**, 021003 (2020).
[33] E.C. Ahn. NPJ 2D Mater. Appl., **4** (1), 1 (2020).
[34] M. Gmitra, J. Fabian. Phys. Rev. B, **92** (15), 155403 (2015).
[35] T. Kampfrath, M. Battiato, P. Maldonado, G. Eilers, J. Nötzold, S. Mährlein, V. Zbarsky, F. Freimuth, Y. Mokrousov, S. Blügel, M. Wolf, I. Radu, P.M. Oppeneer, M. Münzenberg. Nature Nanotechnol., **8** (4), 256 (2013).
[36] E.I. Rashba. Fiz. Tverd. Tela, **2** (6), 1224 (1960). (in Russian).
[37] E. Rashba, A.L. Efros. Appl. Phys. Lett., **83** (25), 5295 (2003).
[38] M. Duckheim, D. Loss. Nature Phys., **2** (3), 195 (2006).
[39] V.K. Dugaev, E.Y. Sherman, J. Barnaś. Phys. Rev. B, **83**, 085306 (2011).
[40] M. Inglot, V.K. Dugaev, E.Y. Sherman, J. Barnaś. Phys. Rev. B, **89**, 155411 (2014).
[41] Yu.A. Bychkov, E.I. Rashba. JETP Lett., **2** (66), 1984 (1973). (in Russian).
[42] S. Konschuh, M. Gmitra, J. Fabian. Phys. Rev. B, **82** (24), 245412 (2010).
[43] M.H.D. Guimaräes, P.J. Zomer, J. Ingla-Aynés, J.C. Brant, N. Tombros, B.J. van Wees. Phys. Rev. Lett., **113**, 086602 (2014).
[44] C.L. Kane, E.J. Mele. Phys. Rev. Lett., **95** (22) (2005).
[45] M. Offidani, M. Milletarı, R. Raimondi, A. Ferreira. Phys. Rev. Lett., **119**, 196801 (2017).
[46] A.W. Cummings, J.H. Garcia, J. Fabian, S. Roche. Phys. Rev. Lett,, **119** (20) (2017).
[47] M. Offidani, R. Raimondi, A. Ferreira. Condens. Matter, **3** (2), 18 (2018).
[48] M.I. Dyakonov (ed.). *Spin Physics in Semiconductors* (Springer, Berlin-Heidelberg, 2008).
[49] K.F. Mak, M.Y. Sfeir, Y. Wu, C.H. Lui, J.A. Misewich, T.F. Heinz. Phys. Rev. Lett., **101** (19) (2008).
[50] Z. Li, E.A. Henriksen, Z. Jiang, Z. Hao, M.C. Martin, P. Kim, H.L. Stormer, D.N. Basov. Nature Physics, **4** (7), 532 (2008).
[51] D.S.L. Abergel, A. Russell, V.I. Fal'ko. Appl. Phys. Lett., **91** (6), 063125 (2007).
[52] L.A. Benítez, J.F. Sierra, W.S. Torres, A. Arrighi, F. Bonell, M.V. Costache, S.O. Valenzuela. Nature Physics, **14** (3), 303 (2017).
[53] M. Johnson, R.H. Silsbee. Phys. Rev. Lett., **55**, 1790 (1985).

*Translated by E.Potapova*